A Trainingless WiFi Fingerprint Positioning Approach Over Mobile Devices

Igor Bisio, *Member, IEEE*, Matteo Cerruti, Fabio Lavagetto, Mario Marchese, *Senior Member, IEEE*, Matteo Pastorino, *Fellow, IEEE*, Andrea Randazzo, *Member, IEEE*, and Andrea Sciarrone, *Member, IEEE*

***Abstract*—Indoor localization of targets by using electromagnetic waves has attracted a lot of attention in the last few years. Thanks to the wide availability of electromagnetic sources deployed for various applications (e.g., WiFi), nowadays it is possible to perform this task by using low-cost mobile devices, such as smartphones. To this end, in order to achieve high positioning accuracy and reduce the computational resources used in the position estimation, fingerprinting approaches are usually employed. However, in this case, a time-consuming training phase, where a great number of measurements must be performed, is needed. In this letter, a novel approach, where the training data are obtained by means of finite-difference time-domain (FDTD) simulations of the electromagnetic propagation in the considered scenario, is presented. The performances of the method are assessed by means of experimental results in a real scenario.**

***Index Terms*—Electromagnetic propagation, fingerprinting, finite-difference time-domain method, indoor positioning.**

I. Introduction

LOCALIZATION of objects by using electromagnetic (EM) waves has attracted a lot of attention in the last few years. In this framework, approaches based on fingerprints (FPs) are often employed since they only need the knowledge of the amplitude of the EM field (which is usually provided by standard mobile apparatuses) to perform the estimation of the position of the target [1]. However, the major problem of fingerprint-based positioning methods is the exhaustive survey needed to train the system, a task that requires substantial cost and time [2]. Another important issue of these systems is that a recalibration is needed every time the environment changes.

The scientific literature highlights the strong needs of methods aimed at reducing the time associated to the offline phase of the FP positioning [3]–[6]. In [3], the need of a method capable of reducing the heavy burden of the training phase is indicated as one of the key challenges in fingerprinting. In [4], it is shown that a valid training phase is hardly bearable since it requires collecting a huge amount of data. To reduce such data, it is proposed to trade position error against time, thus reducing the time needed to train the system [4]. Analogously, it has been pointed out in [5] that a large number of received signal strength (RSS) acquisitions are usually required for calibration and, typically, several hours are necessary to collect such an amount of calibration data. For this reason, it has been stated in [5] that a reduction of the manual effort can be achieved by minimizing the sampling time at each reference point (RP) and/or by limiting the number of locations to sample from. Nevertheless, this simple idea produces inaccurate radio maps, which decrease the accuracy of the location estimation [5].

Attempts of developing training techniques that try to reduce the calibration phase of fingerprint-based systems have been presented in the literature (see for example [7]–[9]). Some works also propose to train the system in an opportunistic way (by using a mobile device such as a smartphone), employing WiFi scans transparently to the user [10]–[12]. Trainingless approaches have been proposed as well. They are based on trilateration solutions [13]–[15], which are computationally heavier and less accurate and reliable than the FP one. In fact, although trilateration does not require any training phase, it is not able to provide the same accuracy, in terms of positioning error, since it does not employ the same amount of information that the FP ones gather during the training phase.

The main contribution of this letter goes in the direction of eliminating the field-training phase. In particular, we propose a WiFi FP indoor positioning system that is trainingless, meaning that the measurement campaign is replaced by an offline phase in which the FPs in each point of the area of interest are estimated by means of EM simulations. In particular, the FP database is constructed offline by simulating the EM field produced by wireless access points (APs) inside the considered scenario by means of the finite-difference time-domain (FDTD) method [16]. The computed electric fields are successively post-processed in order to extract the estimates of the smartphone's received signal strengths, which are used to build the FPs. The combination of these two techniques allows avoiding the burden of the training phase without significantly losing the accuracy of the positioning process. Moreover, it is worth noting that wireless FP localization is often used instead of the multilateration technique since it provides higher positioning accuracy [17]. On the other hand, the multilateration is employed when the applicative environment often changes and time-consuming training phases cannot be repeated each time. Essentially, the approach proposed here allows merging the advantages of the two positioning techniques.

The letter is organized as follows. The proposed approach is described in Section II and validated in Section III by means of a set of experimental test on a real environment. Finally, some conclusions are drawn in Section IV.

Manuscript received September 24, 2013; revised January 31, 2014; accepted April 05, 2014. Date of publication April 11, 2014; date of current version May 06, 2014. *(Corresponding author: Andrea Randazzo.)*

The authors are with the Department of Electrical, Electronic, Telecommunications Engineering, and Naval Architecture, University of Genoa, 16145 Genova, Italy (e-mail: andrea.randazzo@unige.it).

Color versions of one or more of the figures in this letter are available online at http://ieeexplore.ieee.org.

Digital Object Identifier 10.1109/LAWP.2014.2316973

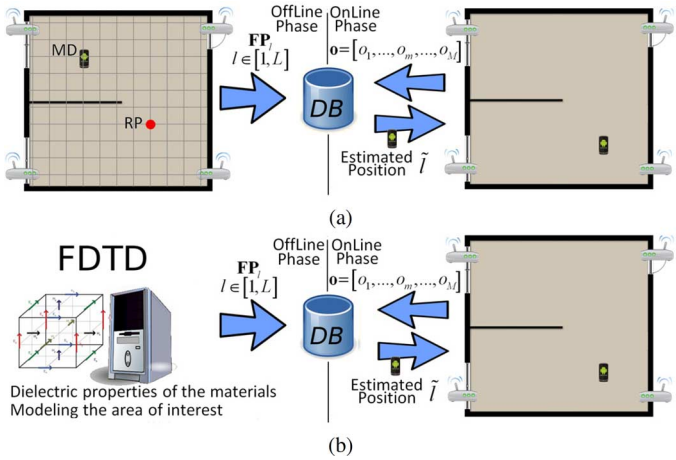

Fig. 1. (a) Traditional and (b) proposed FP architectures.

II. Trainingless Fingerprint Positioning System

This letter proposes a trainingless FP approach. As all the fingerprint methods, it is divided in two phases: a training phase (offline) and a positioning phase (online). All the approaches available in the literature require the mentioned training phase in which the mobile device (MD) measures and stores the power of the received EM field generated by the APs that radiates in the scenario. Operatively, the MD stands still in a set of RPs to measure the RSS, computes the FP associated to the scanned point, and stores it in a reference database (DB). Such a process is iterated until all the RPs have been considered [Fig. 1(a)].

In this letter, such time-consuming training phase is replaced by a computational approach based on an FDTD algorithm [16], which provides a map of the field distribution to be used in order to estimate the RSS values and the corresponding FP in each RP within the area (successively stored in the DB), thus avoiding the time-consuming MD's acquisitions [Fig. 1(b)]. The online positioning phase remains exactly the same as in standard training-based approaches (as detailed in Section II-A).

A. FP Approach

In order to describe the algorithm, we first introduce some notation related to the traditional FP approach present in the literature. L and M represent the RP's and the AP's number, respectively. T is the number of RSS training values acquired every Δt seconds. The index l, $l \in [1, L]$, denotes the generic RP, which is also identified by its coordinates $\mathbf{C}_l = (x_l, y_l)$ defined with respect to a common Cartesian two-dimensional reference system, while m, $m \in [1, M]$, is the index of a single AP. During the offline, or training, phase, a three-dimensional *observation matrix* $\tilde{\mathbf{O}}$ is built. It is composed by L rows and M columns; for each m, l pair, the matrix contains a single observation vector, which includes T RSSs training values. In practice, the element $o_{m,l,t}$, $m \in [1, M]$, $l \in [1, L]$, and $t \in [1, T]$, is the single RSS value received from the mth AP, sensed at the lth RP during the tth signal strength measure. In the training phase of the FP method, the average of the RSS values of each AP, measured in each RP, is used to create the FP database. Analytically, for the lth RP, the vector $\boldsymbol{\mu}_l = [\mu_{1,l}, \ldots, \mu_{m,l}, \ldots, \mu_{M,l}]$ is computed and stored, where each element $\mu_{m,l}$ is calculated as

$$\mu_{m,l} = \frac{1}{T} \sum_{t=1}^{T} o_{m,l,t}. \tag{1}$$

For the lth RP, the vector $\boldsymbol{\mu}_l$ corresponds to the RP's FP $\mathbf{FP}_l = [FP_{1,l}, \ldots, FP_{m,l}, \ldots, FP_{M,l}]$, consequently $\mathbf{FP}_l = \boldsymbol{\mu}_l$. During the online phase, the smartphone acquires the RSS values and computes the observation vector $\mathbf{o} = [o_1, \ldots, o_m, \ldots, o_M]$ by averaging the RSS values acquired from each AP. After that, the distance d_l between $\mathbf{o}$ and each FP $\mathbf{FP}_l$ is computed as reported in the following equation:

$$d_l = \left(\sum_{m=1}^{M} | FP_{m,l} - o_m |^q \right)^{1/q} \tag{2}$$

where q represents the employed norm. In this letter, we fixed $q = 1$. Iterating the calculation reported in (2) for all the L RPs considered in the positioning process allows obtaining the vector $\mathbf{d} = [d_1, \ldots, d_l, \ldots, d_L]$ with $l \in [1, L]$. Finally, the MD's estimated coordinates of the position $\tilde{\mathbf{C}}_l$ are computed by using different criteria, as summarized in Table I. Among them, the so-called nearest neighbor (NN) is the simplest and provides, as MD position, the Cartesian coordinates $\tilde{\mathbf{C}}_l$ of the RP that has the minimum distance d_l. Another simple method is the K-NN, with $K \geq 2$, which averages the coordinates of K RPs with the minimum distances. Finally, the K Weighted Nearest Neighbors, $K \geq 2$ (KW-NN) computes the weighted average of the coordinates of the K RPs with the minimum d_l. In our work, we have considered two different weights $w_l^i = (d_l)^{-i}$, with $i = 1$ and $i = 2$.

TABLE I
MD Position Computing Criteria

NN	$\tilde{\mathbf{C}}_l$ *such that* l: $\arg\min_l\{d_l\}$
K-NN	$\tilde{\mathbf{C}}_l = (\tilde{x}_l, \tilde{y}_l)$ *such that* $\tilde{x}_l = \frac{1}{K}\sum_{k=1}^{K} x_k$, $\tilde{y}_l = \frac{1}{K}\sum_{k=1}^{K} y_k$
KW-NN	$\tilde{\mathbf{C}}_l = (\tilde{x}_l, \tilde{y}_l)$ *such that* $\tilde{x}_l = \frac{1}{\sum_{k=1}^{K} w_k^l}\sum_{k=1}^{K} w_k^l x_k$, $\tilde{y}_l = \frac{1}{\sum_{k=1}^{K} w_k^l}\sum_{k=1}^{K} w_k^l y_k$

B. FDTD-Based Trainingless Approach

The values of the RSS needed to create the database of FPs used in (2) are obtained by means of an EM simulator based on the FDTD method with perfectly matched layer (PML) absorbing boundary conditions [16]. As it is well known, FDTD allows to solve Maxwell equations in order to obtain the EM fields produced by a given source provided that the scenario is known. In this work, the APs have been modeled by using simplified sources (i.e., a line-current source when using the 2-D formulation and a vertical-polarized short dipole in the 3-D case) excited with a unit cosine-modulated Gaussian pulse [16], i.e.,

$$j(t) = \exp[-0.5 t_w^{-2} (t - t_0)^2] \cos\ 2\pi f_0 t. \tag{3}$$

It is worth noting that although the FDTD computation of large-sized domains is clearly time- and memory-consuming, this method is nowadays widely used for field computation inside rooms and buildings [18], [19]. Moreover, it must be considered that in the present application the computation must be performed offline and once for all.

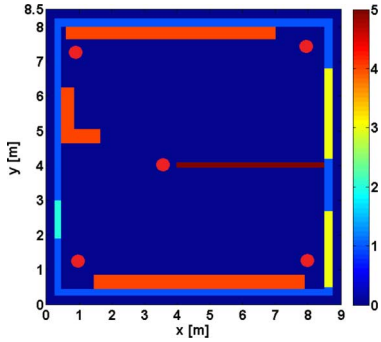

Fig. 2. Cross section of the considered scenario.

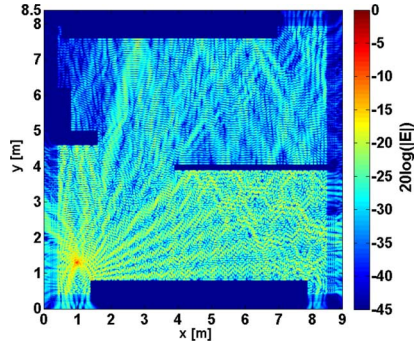

Fig. 3. 2-D FDTD normalized amplitude of the electric field radiated by the first AP inside the considered scenario.

Similarly to the case of indoor WiFi coverage prediction problems, it is assumed that the RSS is approximately proportional to the electric field intensity [20]–[22], which is computed by applying an on-the-fly discrete Fourier transform to the computed time-domain electric field values. Moreover, in order to remove small-scale fading effects, a local mean intensity I is computed. Several approaches have been proposed in the literature for this task. In this letter, I is computed as [20]–[22]

$$l(m,n) = \frac{1}{N^2} \sum_{m'=m-\frac{N-1}{2}}^{m'=m+\frac{N-1}{2}} \sum_{n'=n-\frac{N-1}{2}}^{n'=n+\frac{N-1}{2}} |E_z(m',n')|^2 \tag{4}$$

where N is the size of the averaging window. A similar expression is used for the 3-D case. Similarly to [23], the computed electric field is not calibrated, but it could be scaled with respect to the actual data. Due to the approximations introduced in the propagation modeling, it is difficult to retrieve analytically the scaling parameter. Consequently, an experimental calibration process is employed. In particular, the eventually present scaling factor is computed by minimizing the root mean square error between a set of C calibration measurements and the corresponding simulated values [23].

III. Numerical Results

The developed approach has been tested on a real environment. The considered scenario is an office of dimensions $9 \times 8.5 \times 3$ m^3 containing several pieces of furniture. Two models have been considered: a 2-D one, in which the investigated area is supposed to be of infinite extent along the vertical direction (i.e., a cylindrical symmetry is assumed and the effects of the floor and the ceiling are neglected), and a more detailed 3-D geometry. Fig. 2 shows a cross section of the assumed model (it refers to a height of 1 m for the 3-D case); the colors denote the different objects of the scenario. The values of the dielectric permittivity ϵ_r and of the electric conductivity σ used in the simulations have been chosen according to [24] and are given in Table II, together with the heights of the various parts composing the scenario in the 3-D case.

Five APs, located in the transverse plane at positions (1.05, 1.35), (1.05, 7.20), (7.50, 7.50), (7.50, 1.00), and (3.90, 3.90) m, have been considered (represented by dots in Fig. 2). In the 3-D model, the heights of the APs have been set equal to 2.80 m. The parameters of the source are $f_0 = 2.44$ GHz, $t_w = 1.2 \cdot 10^{-8}$ s, $t_0 = 10\, t_w$. In the FDTD algorithm, the scenario has been discretized with uniform square/cubic subdomains of side 0.005 m (2-D case) and 0.03 (3-D case). Concerning the 3-D case, a coarse discretization has been used in order to reduce the computational time and the memory requirements. In all cases, the time-steps have been computed by applying the Courant criterion [16]. A layer of 10 cells of PML has been considered. The duration of the simulation has been set equal to 500 ns. An example of the computed distribution of the electric field is shown in Fig. 3, which reports the normalized square amplitude of the electric field at the center frequency obtained by FDTD code.

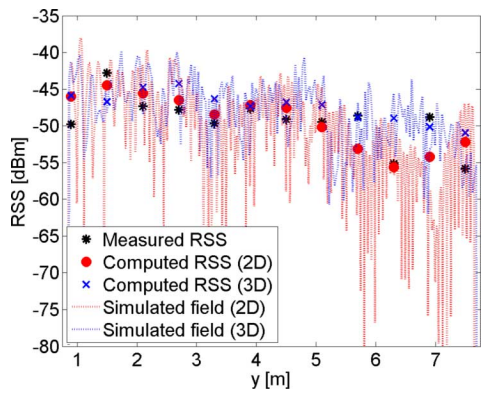

Fig. 4. Comparison of measured and simulated RSS values along a line parallel to y-axis ($x = 1.90$ m).

TABLE II
Dielectric Properties of the Materials Used in the Model

Index	Object	Material	ϵ_r	σ [S/m]	Height
0	Background	Vacuum	1	0	-
1	Wall	Brick	4.5	0.02	3 m
2	Door	Wood	1.5	0	2 m
3	Window	Glass	6	0	1.7 m
4	Locker	Metal	1	10^7	2 m
5	Partition wall	Metal	1	10^7	1.5 m

The electric field map has been processed as described in Section II-B in order to extract the synthetic FPs (an averaging window of side 2.5 λ has been used). In particular, 156 RPs, uniformly distributed on a planar grid with spacing 0.6 m, have been used. For the 3-D case, a horizontal plane at height $z = 1.5$ m has been considered. A set of $C = 5$ measurements, randomly chosen among the set of available measured data, has been used to calibrate the simulated data. An example of the obtained RSS is shown in Fig. 4. Measured data are also provided for comparison.

TABLE III
POSITIONING ERRORS FOR TRAINING AND TRAININGLESS STRATEGIES

	K	Measurements [m]	2D FDTD [m]	3D FDTD [m]
KNN	5	1.58	2.31	2.01
	7	1.61	2.30	2.05
	9	1.60	2.31	2.08
KW-NN	5	1.5	2.29	1.99
	7	1.56	2.29	2.01
	9	1.56	2.31	2.02
KW-NN (quadratic)	5	1.49	2.28	1.97
	7	1.51	2.29	2.00
	9	1.51	2.29	2.02

The obtained databases of FPs are used to estimate the positions of $N = 30$ targets uniformly distributed inside the scenario, and the mean positioning errors have been computed by using the measured and computed FP databases with the different algorithms described in Section II-A. The obtained results are summarized in Table III. As expected, because of the approximations introduced in the model of the scenario, the mean positioning errors obtained in the 2-D and 3-D cases are slightly higher than those obtained with the smartphone measurements. Moreover, the 3-D FDTD algorithm provides lower errors since it allows a better modeling of furniture (especially the partition wall). It is worth noting that, although in the trainingless strategy the errors are higher than those obtained by using the measured FP database, they are still comparable to those available in the literature. Moreover, the decrease in performance is compensated by the gain in terms of training time. Finally, the variation in accuracy due to an inexact knowledge of the scenario has been preliminarily evaluated. To this end, 10 training databases have been generated by using different wall properties (randomly chosen in the ranges $\epsilon_r \in [3, 6]$ and $\sigma \in [0.02, 0.7]$ S/m). By using a 2-D model and the KW-NN strategy with $K = 7$, the estimated positioning error (averaged on the 10 cases) is 2.29 m, whereas the standard deviation is 0.04 m. Similar results have been obtained by using the other strategies. As can be seen, at least in this case, the approach seems to be quite robust to variations in the scenario used in the training stage.

IV. CONCLUSION

In this letter, a trainingless WiFi FP indoor positioning system has been proposed. In the developed approach, the experimental measurement campaign needed to train the positioning algorithm is avoided. The FP database is built offline by computing the EM field produced by the access points in the considered scenario with an FDTD algorithm. The developed strategy has been tested in a real scenario, and the results have been compared to those provided by a standard training procedure, with comparable positioning errors. Further investigations will be devoted to a more extensive analysis of the performances in different scenarios.

REFERENCES

[1] S. A. Zekavat, *Handbook of Position Location Theory, Practice and Advances*. Piscataway, NJ, USA: IEEE Press, 2012.

[2] S. Nikitaki, G. Tsagkatakis, and P. Tsakalides, "Efficient training for fingerprint based positioning using matrix completion," in *Proc. 20th EUSIPCO*, 2012, pp. 195–199.

[3] A. Kushki, K. N. Plataniotis, and A. N. Venetsanopoulos, "Kernel-based positioning in wireless local area networks," *IEEE Trans. Mobile Comput.*, vol. 6, no. 6, pp. 689–705, Jun. 2007.

[4] T. King, T. Haenselmann, and W. Effelsberg, J. Hightower, B. Schiele, and T. Strang, Eds., "Deployment, calibration, and measurement factors for position errors in 802.11-Based indoor positioning systems," in *Proc. 3rd Int. Conf. Location- Context-Awareness*, 2007, pp. 17–34.

[5] X. Chai and Q. Yang, "Reducing the calibration effort for probabilistic indoor location estimation," *IEEE Trans. Mobile Comput.*, vol. 6, no. 6, pp. 649–662, Jun. 2007.

[6] A. Haeberlen, E. Flannery, A. M. Ladd, A. Rudys, D. S. Wallach, and L. E. Kavraki, "Practical robust localization over large-scale 802.11 wireless networks," in *Proc. 10th Annu. Int. Conf. Mobile Comput. Netw.*, New York, NY, USA, 2004, pp. 70–84.

[7] C. Steiner and A. Wittneben, "Efficient training phase for ultra-wideband-based location fingerprinting systems," *IEEE Trans. Signal Process.*, vol. 59, no. 12, pp. 6021–6032, Dec. 2011.

[8] B. Li, J. Salter, A. G. Dempster, and C. Rizos, "Indoor positioning techniques based on wireless LAN," in *Proc. 1st IEEE Int. Conf. Wireless Broadband Ultra Wideband Commun.*, Sydney, Australia, 2006, pp. 13–16.

[9] Z. Yang, C. Wu, and Y. Liu, "Locating in fingerprint space: Wireless indoor localization with little human intervention," in *Proc. 18th Annu. Int. Conf. Mobile Comput. Netw.*, New York, NY, USA, 2012, pp. 269–280.

[10] J. Lathouwers, M. Weyn, and C. Vercauteren, "User-trained, zero-configuration, self-adaptive opportunistic Wi-Fi localization for room-level accuracy," in *Proc. 2nd AMBIENT*, Barcelona, Spain, 2012, pp. 64–70.

[11] Y. Chon, N. D. Lane, F. Li, H. Cha, and F. Zhao, "Automatically characterizing places with opportunistic crowdsensing using smartphones," in *Proc. ACM Conf. Ubiquitous Comput.*, Pittsburgh, PA, 2012, pp. 481–490.

[12] I. Bisio, F. Lavagetto, M. Marchese, and A. Sciarrone, "GPS/HPS-and Wi-Fi fingerprint-based location recognition for check-in applications over smartphones in cloud-based LBSs," *IEEE Trans. Multimedia*, vol. 15, no. 4, pp. 858–869, Jun. 2013.

[13] K. Chintalapudi, A. P. Iyer, and V. N. Padmanabhan, "Indoor localization without the pain," in *Proc. 16th Annu. Int. Conf. Mobile Comput. Netw.*, Chicago, IL, USA, 2010, pp. 173–184.

[14] L. F. M. de Moraes and B. A. A. Nunes, "Calibration-free WLAN location system based on dynamic mapping of signal strength," in *Proc. 4th ACM Int. Workshop Mobile Manag. Wireless Access*, New York, NY, USA, 2006, pp. 92–99.

[15] H. Lim, L.-C. Kung, J. C. Hou, and H. Luo, "Zero-Configuration indoor localization over IEEE 802.11 wireless infrastructure," *Wireless Netw.*, vol. 16, no. 2, pp. 405–420, Feb. 2010.

[16] A. Taflove and S. C. Hagness, *Computational Electrodynamics: The Finite-Difference Time-Domain Method*. Boston, MA, USA: Artech House, 2005.

[17] J. Kwon, B. Dundar, and P. Varaiya, "Hybrid algorithm for indoor positioning using wireless LAN," in *Proc. 60th IEEE Veh. Technol. Conf.*, Los Angeles, CA, USA, 2004, pp. 4625–4629.

[18] L. Talbi and G. Y. Delisle, "Finite difference time domain characterization of indoor radio propagation," *Prog. Electromagn. Res.*, vol. 12, pp. 251–275, 1996.

[19] A. C. M. Austin, M. J. Neve, and G. B. Rowe, "Modeling propagation in multifloor buildings using the FDTD method," *IEEE Trans. Antennas Propag.*, vol. 59, no. 11, pp. 4239–4246, Nov. 2011.

[20] J.-M. Gorce, K. Jaffres-Runser, and G. d. l. Roche, "Deterministic approach for fast simulations of indoor radio wave propagation," *IEEE Trans. Antennas Propag.*, vol. 55, no. 3, pp. 938–948, Mar. 2007.

[21] T. T. Zygiridis *et al.*, "Numerical modeling of an indoor wireless environment for the performance evaluation of WLAN systems," *IEEE Trans. Magn.*, vol. 42, no. 4, pp. 839–842, Apr. 2006.

[22] Z. Yun, M. F. Iskander, and Z. Zhang, "Complex-Wall effect on propagation characteristics and mimo capacities for an indoor wireless communication environment," *IEEE Trans. Antennas Propag.*, vol. 52, no. 4, pp. 914–922, Apr. 2004.

[23] K. Runser and J.-M. Gorce, "Assessment of a new indoor propagation prediction method based on a multi-resolution algorithm," in *Proc. 61st IEEE Veh. Technol. Conf.*, Stockholm, Sweden, 2005, pp. 35–38.

[24] S. Stavrou and S. R. Saunders, "Review of constitutive parameters of building materials," in *Proc. 12th Int. Conf. Antennas Propag.*, Exeter, U.K., 2003, vol. 1, pp. 211–215.